

## Research Article

# Thermoluminescence and Photoluminescence Study of Erbium Doped $\text{CaY}_2\text{O}_4$ Phosphor

Vikas Dubey,<sup>1</sup> Ratnesh Tiwari,<sup>1</sup> Raunak Kumar Tamrakar,<sup>2</sup> Chandrabhushan Markande,<sup>1</sup> Gajendra Singh Rathore,<sup>3</sup> and Mahendra Kumar Pradhan<sup>3</sup>

<sup>1</sup>Department of Physics, Bhilai Institute of Technology, Raipur 493661, India

<sup>2</sup>Department of Physics, Bhilai Institute of Technology, Durg 491001, India

<sup>3</sup>Department of Electronics and Communication, School of Engineering and IT, MATS University, University Campus, Arang-Kharora Highway, Gullu, Raipur 493441, India

Correspondence should be addressed to Vikas Dubey; [jsvikasdubey@gmail.com](mailto:jsvikasdubey@gmail.com)

Received 31 May 2015; Revised 1 September 2015; Accepted 6 September 2015

Academic Editor: Fernando Rubio-Marcos

Copyright © 2015 Vikas Dubey et al. This is an open access article distributed under the Creative Commons Attribution License, which permits unrestricted use, distribution, and reproduction in any medium, provided the original work is properly cited.

Phosphor doped with erbium ion with variable concentration (0.5–2 mol%) was synthesized by solid state reaction method.  $\text{CaY}_2\text{O}_4:\text{Er}^{3+}$  phosphor is characterized by X-ray diffraction technique for structural analysis and crystallite size calculation. Average crystallite size was found to be nearly 58 nm. Two prominent TL glow peaks found at 163°C associated with higher temperature peak 340°C. The peak intensity of higher temperature (340°C) peak was less as compared to lower temperature peak (163°C) because the deep trapping formation is less in case of UV irradiation. Sample shows good TL glow curve and for variable UV exposure time maximum TL intensity was found at 20 min UV exposure which is optimized UV exposure time. Sample was studied by photoluminescence emission spectra excited by xenon flash lamp with nearly 360 nm and four prominent peaks found at wavelengths 445, 525, 553, and 565 nm; here the 445 and 565 nm peak were intense as compared to others. From the PL emission spectra, it is concluded that the color tenability of prepared  $\text{CaY}_2\text{O}_4:\text{Er}^{3+}$  was blue-green and it is verified by CIE coordinate. Kinetic parameters of prepared phosphor were calculated by computerized glow curve deconvolution (CGCD) technique.

## 1. Introduction

In recent years, practical applications in optical devices, such as color display, optical data storage, biomedical diagnostics, and temperature sensors, have been produced on the basis of rare earth ion doped materials [1, 2]. Recently, the luminescence properties of rare earth ions in  $\text{CaY}_2\text{O}_4$  have attracted much attention.  $\text{CaY}_2\text{O}_4$  belongs to the ordered  $\text{CaFe}_2\text{O}_4$  structure, which is composed of a  $(\text{R}_2\text{O}_4)_2$  (R is rare earth metal) framework of double octahedral structure with rare earth ions residing within the framework. Due to the thermal and chemical stability,  $\text{CaY}_2\text{O}_4$  has been used in thermal barrier coating (TBC) materials [3, 4].

The paper describes synthesis of rare earth doped phosphor which may be applicable for display devices applications. The object of the present investigation is to report the results of luminescence studies in terms of photoluminescence and thermoluminescence properties of  $\text{CaY}_2\text{O}_4:\text{Er}^{3+}$

phosphor with variable concentration of erbium ions. To the best of our knowledge and on the basis of literature survey suggestions, it is claimed that this paper attempts to address the PL and TL studies for the first time.

## 2. Experimental

Preparing  $\text{CaY}_2\text{O}_4$  phosphor with erbium (0.5–2 mol%) which consists of heating stoichiometric amounts of reactant mixture is taken in alumina crucible for calcination at 1000°C temperature, and sintering temperature was 1300°C for 4 hours in a muffle furnace. Every heating is followed by intermediate grinding using agate mortar and pestle. The Er activated  $\text{CaY}_2\text{O}_4$  phosphor was prepared via high temperature modified solid state diffusion. The starting materials were as follows:  $\text{Y}_2\text{O}_3$ ,  $\text{CaCO}_3$ ,  $\text{Er}_2\text{O}_3$ , and  $\text{H}_2\text{BO}_3$  (as a flux) in molar ratio used to prepare the phosphor [5].

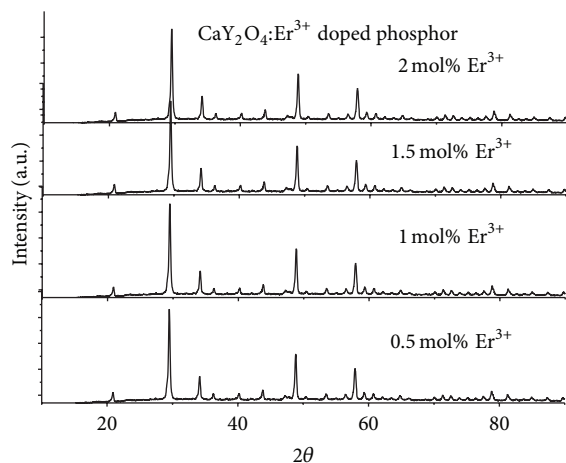


FIGURE 1: XRD pattern of  $\text{CaY}_2\text{O}_4:\text{Er}^{3+}$  (0.5–2 mol%).

The sample was characterized using photoluminescence (PL), thermoluminescence (TL), XRD, FEGSEM, and HRTEM. The XRD measurements were carried out using Bruker D8 Advance X-ray diffractometer. The X-rays were produced using a sealed tube and the wavelength of X-ray was 0.154 nm (Cu K-alpha). The X-rays were detected using a fast counting detector based on Silicon strip technology (Bruker Lynx Eye Detector). Observation of particle morphology was investigated by FEGSEM (field emission gun scanning electron microscope) (JEOL JSM-6360). The photoluminescence (PL) emission and excitation spectra were recorded at room temperature by use of a Shimadzu RF-5301 PC spectrofluorophotometer. The excitation source was a xenon lamp. Thermally stimulated luminescence glow curves were recorded at room temperature by using TLD reader I1009 supplied by Nucleonix Sys. Pvt. Ltd., Hyderabad. The obtained phosphor under the TL examination is given UV radiation using 254 nm UV source [6].

### 3. Results and Discussion

The prepared phosphor materials were analysed by XRD to reveal phase compositions and the crystallite size (Figure 1). The crystallite size was calculated from the XRD pattern following the Scherer equation  $D = 0.9\lambda/\beta \cos\theta$ . Here,  $D$  is the crystallite size for the  $(hkl)$  plane,  $\lambda$  is the wavelength of the incident X-ray radiation [CuK $\alpha$  (0.154056 nm)],  $\beta$  is the full width at half maximum (FWHM) in radians, and  $\theta$  is the diffraction angle for the  $(hkl)$  plane. From the XRD pattern, it was found that the prominent phase formed is  $\text{CaY}_2\text{O}_4$ . This reveals that the structure of  $\text{CaY}_2\text{O}_4$  is orthorhombic. For variable erbium concentration, it is found that from the XRD pattern there is no impurity phase. For XRD pattern, corresponding miller indices values are calculated, which matches with JCPDS card number. Sample shows orthorhombic structure. The crystallite size calculated using Scherer's formula is 56.41 nm.

SEM micrographs are recorded for 10000x resolution of prepared sample. Figure 2 of the SEM micrographs of  $\text{CaY}_2\text{O}_4:\text{Er}$  (1%) indicates clearly that the particles are of

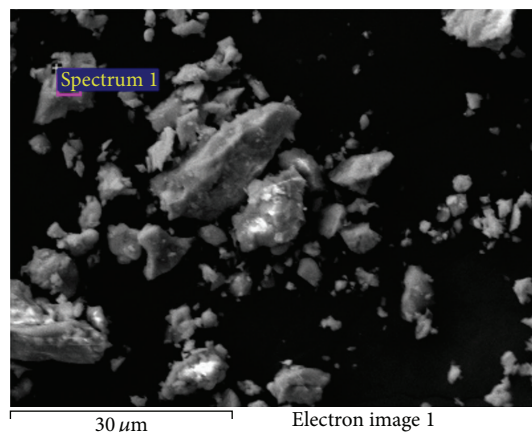


FIGURE 2: SEM image of prepared phosphor.

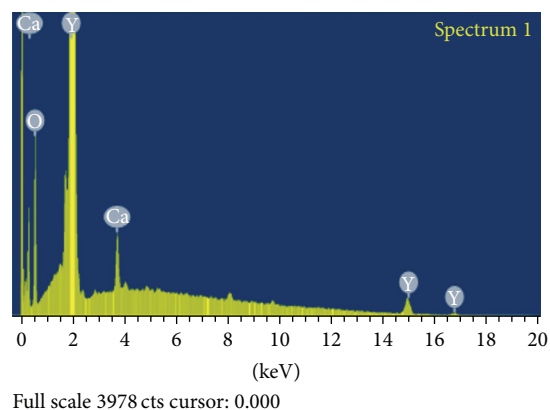


FIGURE 3: EDX analysis of  $\text{CaY}_2\text{O}_4$  phosphor.

uniform size having good connectivity with grain. The average particles have shown microflowers with the particle size of 55 nanometer-few microns. From the elemental analysis, it is found that intense Ca, Y, and O ions are present in the sample (Figure 3). EDX pattern also confirms the formation of  $\text{CaY}_2\text{O}_4$  phosphor.

FTIR spectrum of  $\text{CaY}_2\text{O}_4:\text{Er}$  (1%) phosphor is shown in Figure 4. This spectrum expresses strong broad peaks at  $412\text{ cm}^{-1}$  to  $446\text{ cm}^{-1}$  which are the characteristics of Y-O vibrations. Presence of Ca-O gives rise to an IR peak within a range of  $1265\text{ cm}^{-1}$ . All these observed peaks found together confirm the formation of  $\text{CaY}_2\text{O}_4$  phosphor. From the FTIR spectrum, it is observed that the peak at  $\sim 3643\text{ cm}^{-1}$  is assigned to intermolecular H bonding of  $\text{H}_2\text{O}$ . The specimen might have absorbed moisture from the atmosphere.

The TL glow curve of  $\text{CaY}_2\text{O}_4$  phosphor doped erbium ions shows broad TL glow curve. It is centered at  $163^\circ\text{C}$  having shoulder peak at  $340^\circ\text{C}$ . It shows linear response with UV dose (Figure 5). TL intensity increases with increasing UV exposure time (inset of Figure 6) and peak centered at  $163^\circ\text{C}$  which shows good peak for thermoluminescence dosimeter peak. When this curve is fitted by CGCD technique it shows good theoretical and experimental fit for the same analysis of different authors [7, 8].

TABLE 1: Calculation of kinetic parameter for CGCD curve.

Peaks	$T_1$ °C	$T_m$ °C	$T_2$ °C	$\tau$	$\delta$	$\omega$	$\mu = \delta/\omega$	Activation energy	Frequency factor
1	120	157	187	37	30	67	0.448	0.636	$3 \times 10^8$
2	165	216	252	51	36	87	0.414	0.587	$9 \times 10^6$
3	269	335	397	66	62	128	0.484	0.716	$5 \times 10^6$

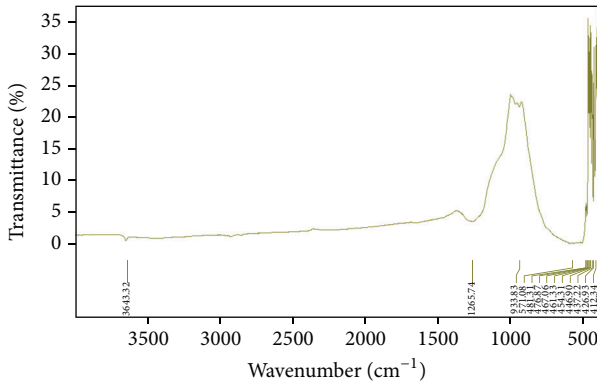
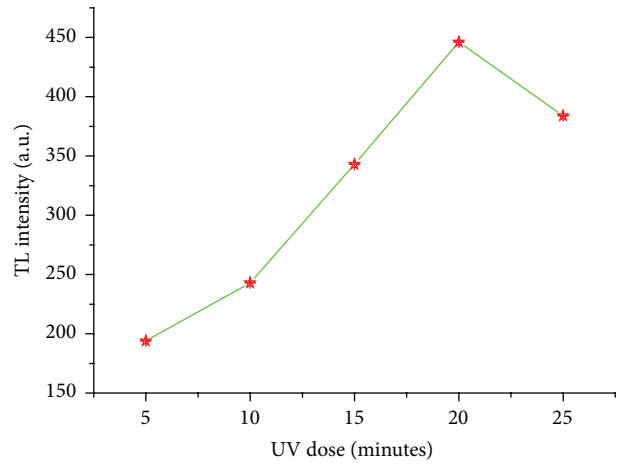


FIGURE 4: FTIR spectra of prepared phosphor.



—\*— Dose versus intensity

FIGURE 6: Doses versus intensity plot for UV exposure time.

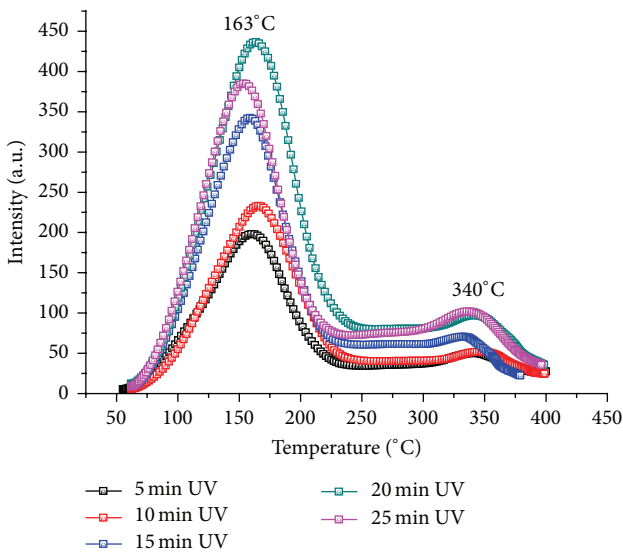


FIGURE 5: TL glow curve analysis of prepared phosphor.

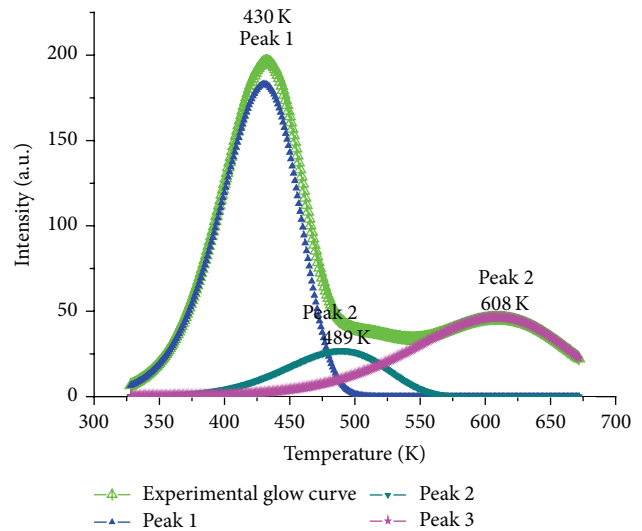


FIGURE 7: CGCD curve for comparative study.

From CGCD pattern clearly broad 3 peaks centered at 430 K, 489 K, and 608°C (Figure 7) and for these three peaks kinetic parameters are calculated (Table 1). Here the TL glow curve shows good agreement with UV dose and shows linear response with high temperature peak which gives the information about dosimetric loss in the prepared phosphor. The peak centered at 163° is due to formation of shallower trap and 340°C peak is due to deeper trap.

From the calculated kinetic parameters, it is found that glow curve is characteristic of the different trap levels that lie in the band gap of the material. A reliable dosimetric study of a thermoluminescent material should be based on good

knowledge of its kinetic parameters that include trap depth ( $E$ ), order of kinetics ( $b$ ), and frequency factor ( $s$ ). The study of relatively deep trapping defect-states in various phosphors, as well as TL dating of solid state materials, is closely related to the position of the trapping levels within the forbidden gap. However, there are various methods to obtain the number of glow peaks in the complex glow curves and their kinetic parameters that best describe the peaks [9–11]. Here the order of kinetics shows general order which nearly goes to second

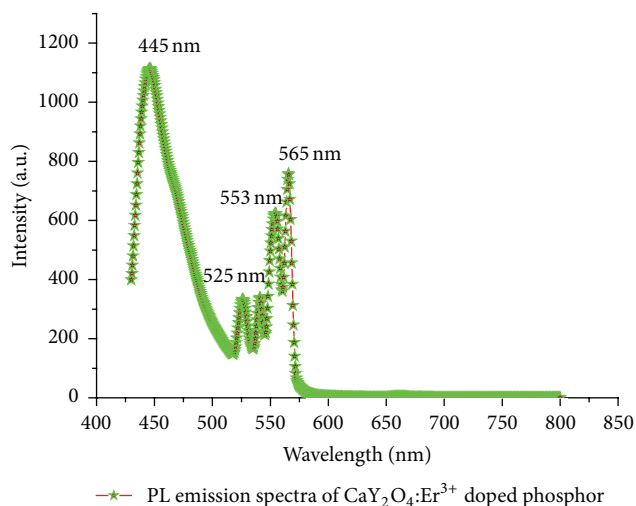


FIGURE 8: PL emission spectra for  $\text{CaY}_2\text{O}_4$  phosphor doped with erbium ion.

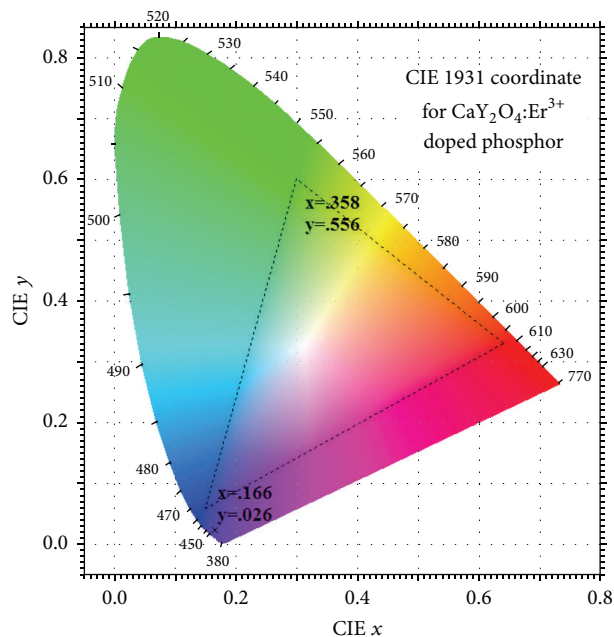


FIGURE 9: CIE 1931 coordinate for  $\text{CaY}_2\text{O}_4$  phosphor doped with erbium ion (blue-green emission).

order. Activation energy is found highest for higher peak and varies from three peaks: 0.63, 0.58, and 0.71 eV.

Prepared phosphor was studied by photoluminescence analysis; it is found that the emission spectra with  $\text{Er}^{3+}$  show strong peaks at 445 nm, 525 nm, 553 nm, and 565 nm range (Figure 8), the dominant peak at 445 nm due to the ( $^2\text{H}_{11/2}$ ,  $^4\text{S}_{3/2}$ ) transition, and weaker transition at 565 nm with peak associated with 525 and 553 nm. Spectrophotometric determinations of peaks are evaluated by Commission Internationale de l'Éclairage (CIE) technique (Figure 9).

The CIE coordinates were calculated by spectrophotometric method using the spectral energy distribution [12–16]

of the  $\text{CaY}_2\text{O}_4:\text{Er}^{3+}$  sample (Figure 9). The color coordinates for the  $\text{Er}^{3+}$  doped sample are  $x = 0.358$  and  $y = 0.556$  (these coordinates are very near to the green light emission) and  $x = 0.166$  and  $y = 0.026$  (these coordinates are very near to the blue light emission). Hence this phosphor has excellent color tenability from blue-green light emission. So the prepared phosphor may be useful for blue-green emissions for display application [17, 18].

## 4. Conclusion

The samples were prepared by solid state synthesis technique which is suitable for large scale production for phosphors. From XRD study, the prepared sample has orthorhombic structure and no impurity phase was found in XRD. The calculated particle size by Scherer's formula was found to be 58 nm. The surface morphology of prepared phosphor shows compact distribution with some agglomerates. The emission spectra with constant concentration of  $\text{Er}^{3+}$  show strong peaks at 445 nm, 525 nm, 553 nm, and 565 nm, the dominant peak at 445 nm due to the ( $^2\text{H}_{11/2}$ ,  $^4\text{S}_{3/2}$ ) transition, and weaker transition at 525 nm, 553 nm, and 565 nm. Spectrophotometric determinations of peaks are evaluated by Commission Internationale de l'Éclairage (CIE) technique. It shows the color tenability near blue-green emission so the prepared phosphor is useful for display device applications for blue-green emission. TL glow curve analysis and CGCD pattern of TL glow curve determine the kinetic parameters, which gives information about dosimetric loss in the material. Here the order of kinetics shows general order which nearly goes to second order. Activation energy is found to be the highest for higher peak and varies from three peaks: 0.63, 0.58, and 0.71 eV. High temperature TL glow peak shows more stability and less fading of the behaviour displayed by phosphor is useful for dosimetric application.

## Conflict of Interests

The authors declare that there is no conflict of interests regarding the publication of this paper.

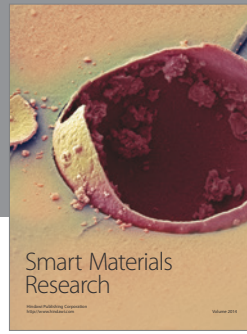
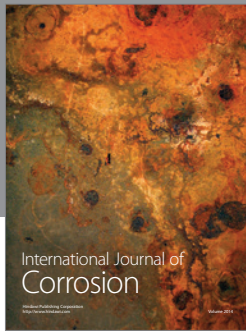
## Acknowledgments

The authors are very thankful for Chhattisgarh Council of Science and Technology funding through Mini-Research Project and are also thankful for Professor M. M. Hambarde, Director General of CCOST.

## References

- [1] J. H. Yang, L. Y. Zhang, L. Wen, S. X. Dai, L. L. Hu, and Z. H. Jiang, "Optical transitions and upconversion luminescence of  $\text{Er}^{3+}/\text{Yb}^{3+}$ -codoped halide modified tellurite glasses," *Journal of Applied Physics*, vol. 95, no. 6, pp. 3020–3026, 2004.
- [2] S. F. Lim, R. Riehn, W. S. Ryu et al., "In vivo and scanning electron microscopy imaging of upconverting nanophosphors in *Caenorhabditis elegans*," *Nano Letters*, vol. 6, no. 2, pp. 169–174, 2006.

- [3] K. Kurosaki, T. Tanaka, T. Maekawa, and S. Yamanaka, "Thermal properties of polycrystalline sintered  $\text{SrY}_2\text{O}_4$ ," *Journal of Alloys and Compounds*, vol. 395, no. 1-2, pp. 318–321, 2005.
- [4] K. Kurosaki, T. Tanaka, T. Maekawa, and S. Yamanaka, "Thermophysical properties of  $\text{SrY}_2\text{O}_4$ ," *Journal of Alloys and Compounds*, vol. 398, no. 1-2, pp. 304–308, 2005.
- [5] V. Dubey, J. Kaur, and S. Agrawal, "Effect of europium concentration on photoluminescence and thermoluminescence behavior of  $\text{Y}_2\text{O}_3:\text{Eu}^{3+}$  phosphor," *Research on Chemical Intermediates*, vol. 41, no. 7, pp. 4727–4739, 2015.
- [6] V. Dubey, J. Kaur, S. Agrawal, N. S. Suryanarayana, and K. V. R. Murthy, "Effect of  $\text{Eu}^{3+}$  concentration on photoluminescence and thermoluminescence behavior of  $\text{YBO}_3:\text{Eu}^{3+}$  phosphor," *Superlattices and Microstructures*, vol. 67, pp. 156–171, 2014.
- [7] Y. Zorenko, V. Gorbenko, V. Savchyn et al., "Scintillation and luminescent properties of undoped and  $\text{Ce}^{3+}$  doped  $\text{Y}_2\text{SiO}_5$  and  $\text{Lu}_2\text{SiO}_5$  single crystalline films grown by LPE method," *Optical Materials*, vol. 34, no. 12, pp. 1969–1974, 2012.
- [8] E. Zych, A. Zych, J. Zhang, and S. Wang, "New fabrication procedure of  $\text{Y}_2\text{SiO}_5:\text{Ce}$  and its structural and spectroscopic characterization," *Journal of Alloys and Compounds*, vol. 451, no. 1-2, pp. 286–289, 2008.
- [9] V. Dubey, J. Kaur, and S. Agrawal, "Effect of europium concentration on photoluminescence and thermoluminescence behavior of  $\text{Y}_2\text{O}_3:\text{Eu}^{3+}$  phosphor," *Research on Chemical Intermediates*, vol. 41, no. 7, pp. 4727–4739, 2015.
- [10] D. W. Cooke, J. K. Lee, B. L. Bennett, J. R. Grovers, and L. G. Jacobsohn, "Luminescent properties and reduced dimensional behavior of hydrothermally prepared  $\text{Y}_2\text{SiO}_5:\text{Ce}$  nanophosphors," *Applied Physics Letters*, vol. 88, Article ID 103108, 2006.
- [11] C. F. Yan, G. J. Zhao, Y. Hang, L. H. Zhang, and J. Xu, "Comparison of cerium-doped  $\text{Lu}_2\text{Si}_2\text{O}_7$  and  $\text{Lu}_2\text{SiO}_5$  scintillators," *Journal of Crystal Growth*, vol. 281, no. 2–4, pp. 411–415, 2005.
- [12] V. Dubey, S. Agrawal, and J. Kaur, "Photoluminescence and thermoluminescence behavior of Gd doped  $\text{Y}_2\text{O}_3$  phosphor," *Optik—International Journal for Light and Electron Optics*, vol. 126, no. 1, pp. 1–5, 2015.
- [13] V. Dubey, J. Kaur, and S. Agrawal, "Effect of europium doping levels on photoluminescence and thermoluminescence of strontium yttrium oxide phosphor," *Materials Science in Semiconductor Processing*, vol. 31, pp. 27–37, 2015.
- [14] V. Dubey, J. Kaur, and S. Agrawal, "Synthesis and characterization of  $\text{Eu}^{3+}$ -doped  $\text{Y}_2\text{O}_3$  phosphor," *Research on Chemical Intermediates*, vol. 41, no. 1, pp. 401–408, 2015.
- [15] V. Dubey, J. Kaur, N. S. Suryanarayana, and K. V. R. Murthy, "Thermoluminescence study, including the effect of heating rate, and chemical characterization of Amarnath stone collected from Amarnath Holy Cave," *Research on Chemical Intermediates*, vol. 40, no. 2, pp. 531–536, 2014.
- [16] V. Dubey, J. Kaur, N. S. Suryanarayana, and K. V. R. Murthy, "Thermoluminescence and chemical characterization of natural calcite collected from Kodwa mines," *Research on Chemical Intermediates*, vol. 39, no. 8, pp. 3689–3697, 2013.
- [17] Y. Parganiha, J. Kaur, V. Dubey, and K. V. R. Murthy, "Near UV-blue emission from Ce doped  $\text{Y}_2\text{SiO}_5$  phosphor," *Materials Science in Semiconductor Processing*, vol. 31, pp. 715–719, 2015.
- [18] C. Hu, H. Liu, W. Dong et al., " $\text{La}(\text{OH})_3$  and  $\text{La}_2\text{O}_3$  nanobelts-synthesis and physical properties," *Advanced Materials*, vol. 19, no. 3, pp. 470–474, 2007.



**Hindawi**

Submit your manuscripts at  
<http://www.hindawi.com>

